Desalination and Water Treatment
www.deswater.com

doi: 10.5004/dwt.2017.21058

81 (2017) 170–185
June

Comparative study on photocatalytic treatment of diclofenac: slurry vs. immobilized processes

Daria Juretic Perisic[a], Alexandre Belet[a,b], Hrvoje Kusic[a,*], Urska Lavrencic Stangar[c], Ana Loncaric Bozic[a,*]

[a]*Faculty of Chemical Engineering and Technology, University of Zagreb, Marulicev trg 19, Zagreb 10000, Croatia, Tel. +385 1 4597 160; Fax: +385 1 4597 143; email: hkusic@fkit.hr (H. Kusic), Tel. +385 1 4597 123; Fax: +385 1 4597 143; email: abozic@fkit.hr (A.L. Bozic)*
[b]*National Polytechnic Institute of Industrial and Chemical Engineering, Toulouse, France*
[c]*Laboratory for Environmental Research, University of Nova Gorica, Vipavska 13, SI-5000 Nova Gorica, Slovenia*

Received 21 February 2017; Accepted 17 June 2017

ABSTRACT

The applicability of different photocatalytic systems for the treatment of pharmaceuticals in water was investigated. Slurry (UV-A/TiO_2(s) and UV-A/TiO_2(s)/H_2O_2) and immobilized (UV-A/TiO_2(i)/H_2O_2) processes were compared regarding the removal of diclofenac (DCF) and total organic content, as well as the improvements in biodegradability and toxicity. The applied response surface modeling revealed the significance of TiO_2 dosage and concentration of H_2O_2, while pH was less influential within the studied range. Although UV-A/TiO_2(i)/H_2O_2 was somewhat less effective in comparison with UV-A/TiO_2(s)/H_2O_2 process (88.8% and 99.1% of DCF removal, respectively), the immobilized system enabled photocatalyst reuse. In comparison with air dried and thermally reactivated, chemically reactivated photocatalyst provided better performance through four consecutive runs.

Keywords: TiO_2 photocatalysis; Pharmaceuticals; Slurry process; Immobilized photocatalyst; Reactivation

1. Introduction

Untreated wastewaters represent a serious threat as they contain various types of pollutants. Even when applying wastewater treatment (WWT) methods, various pollutants may be present upon achieving effluent guidelines. Nowadays, the occurrence of chemicals like pharmaceuticals, detergents, and personal care products in the environment due to the everyday human routine as bathing, cleaning, medical care, and human waste disposal, represents a growing problem [1]. Conventional WWT methods are not specifically designed for their removal and consequently these chemicals are detected in high ng L^{-1} to low μg L^{-1} concentrations in the WWT plant effluents [2]. Diclofenac (DCF) is one of three pharmaceuticals added to "watch list" of priority substances in water [3]. DCF is active compound in a numerous commercially available drugs and one of the most used worldwide, with an estimated annual consumption of 940 t [4]. After the therapeutic use, 15% of DCF is excreted from the human organism in unchanged form [5], reaching municipal wastewater. Due to insufficient treatment in WWT plants [5–8], DCF is detected in surface waters in concentrations that may represent potential harm to health and the environment [5].

The need for effective and environmentally and economically viable treatment of pharmaceuticals is in the focus of nowadays research. Advanced oxidation processes (AOPs) have shown to be efficient for degradation of persistent, non-biodegradable, and toxic compounds in the water matrix [9]. Among AOPs, heterogeneous photocatalytic processes present the promising solution due to their ability to degrade pharmaceuticals and lower the toxicity and upraise biodegradability of treated water [10–13]. Nano-TiO_2 is one of the most researched photocatalyst characterized

* Corresponding author.

by excellent mechanical and chemical properties. It can be activated by irradiation wavelengths below 390 nm. Taking into account that solar spectrum comprise of 5% of UV-A, usage of nano-TiO_2 enable harvesting of solar irradiation in photocatalytic water treatment [14–17]. On the other hand, the application of TiO_2-nanoparticles in water treatment is impractical due to in-treatment agglomeration and demanding post-treatment separation [15]. To overcome these disadvantages, the immobilization of nanoparticles can be applied [18]. The main challenges associated with the processes utilizing immobilized photocatalyst are the preservation of high surface area and its activity during treatment, and the stability of immobilized catalyst's layers to be applied in consecutive runs [15].

In this study, nano-TiO_2 photocatalytic processes were applied for the removal of DCF from aqueous solution. The investigated processes involved TiO_2 being suspended in a slurry using UV-A irradiation without and with the addition of oxidant (UV-A/TiO_2(s) and UV-A/TiO_2(s)/H_2O_2, respectively), and immobilized TiO_2 on glass substrates with the addition of oxidant (UV-A/TiO_2(i)/H_2O_2). Operating parameters of the applied photocatalytic treatments: (i) initial pH; (ii) catalyst dosage in terms of catalyst mass concentration for slurry and number of layers for immobilized film; and (iii) oxidant concentration (where added), were investigated. Design of experiments with response surface modeling (RSM) was employed to estimate the influence of studied parameters on DCF removal by applied photocatalytic processes. The environmental aspects of the applied photocatalytic treatments were evaluated on the basis of mineralization extent, changes in biodegradability, and toxicity. In process using immobilized photocatalyst, its reuse in consecutive cycles upon chemical and thermal reactivation was examined.

2. Materials and methods

2.1. Chemicals

2-[(2,6-Dichlorophenyl)amino]benzeneacetic acid sodium salt (DCF) was purchased from Sigma-Aldrich, USA, and used as a model water pollutant. The constituents of mobile phase used in high-performance liquid chromatography (HPLC) were: methanol (CH_3OH, HPLC grade, J.T. Baker, The Netherlands) and *ortho*-phosphoric acid (*o*-H_3PO_4, >85%, Sigma-Aldrich, USA). Titanium(IV) oxide (AEROXIDE TiO_2 P25, Evonik, USA) was used as a catalyst in a slurry system. For TiO_2 thin-film preparation the following chemicals were used: Levasile® 200/30 (colloidal SiO_2, Obermeier, Germany), tetraethyl orthosilicate (TEOS, $Si(OC_2H_5)_4$, 99% GC grade, Sigma-Aldrich, USA), titanium tetraisopropoxide (TTIP, $(Ti\{OCH(CH_3)_2\}_4$, 97%, Sigma-Aldrich, USA), hydrochloric acid (HCl, 36.5%, Gram-mol, Croatia), perchloric acid ($HClO_4$, 70%, Kemika, Croatia), and ethanol (EtOH, C_3H_5OH, 99.8%, Sigma-Aldrich, USA). Hydrogen peroxide (H_2O_2, w = 30%, Kemika, Croatia) was used as an oxidant. The following auxiliary chemicals were used as well: sodium hydroxide (NaOH, p.a., Kemika, Croatia), sulfuric acid (H_2SO_4, >96%, Kemika, Croatia), sodium chloride (NaCl, p.a., Kemika, Croatia), and sodium sulfite (Na_2SO_3, p.a., Keimika, Croatia). Deionized water with conductivity less than 1 μS cm^{-1} was used in all experiments.

2.2. Photocatalysts immobilization

TiO_2 thin films were prepared according to the procedure by Kete et al. [19]. Hydrolysis of TTIP in aqueous EtOH acidified with $HClO_4$, during reflux for 48 h, resulted in the formation of nanocrystalline titania sol (SOL1). A separate homogenous silica sol (SOL2) was prepared by intensive mixing of TEOS, deionized water, and HCl for 1 h. The binder sol was prepared by stepwise addition of SOL2, colloidal SiO_2 (i.e., Levasil) and EtOH to nanocrystalline titania sol (SOL1). AEROXIDE TiO_2 P25 was added to the binder sol and homogenized in ultrasonic bath for 10 min. Thin-film layers were immobilized on glass plates, dimensions of 0.9 × 10 × 2 mm, by dip-coating technique using a in-house made laboratory dip coater. The immersion speed for the dip coating was 10 cm min^{-1}. After deposition, the layer was dried by hot air, and then treated in a laboratory furnace at 200°C for 1 h. The described procedure was repeated in order to obtain desired number of thin-film layers.

2.3. Photocatalytic experiments with slurry and immobilized TiO_2

UV-A/TiO_2(s), UV-A/TiO_2(s)/H_2O_2, and UV-A/TiO_2(i)/H_2O_2 were carried in a glass batch reactor (V = 0.1 L), equipped with magnetic stirrer, to treat 0.1 mM DCF aqueous solution. The reaction temperature (T = 25°C ± 0.2°C) was maintained by immersing the reactor in a flow-through water cooling bath. An UV-A low pressure mercury lamp, UVP-Ultra Violet Products, UK, was placed in the middle of the reactor in a quartz tube and used as an irradiation source. The pH value of DCF aqueous solution was adjusted using 0.01 M NaOH and 0.01 M H_2SO_4, followed by the addition of TiO_2 and H_2O_2 (where needed) according to the experimental plan (Tables 1 and S1–S3). In slurry processes, the demanded dosage of nano-TiO_2 powder was added, while in the immobilized system, the plates with certain number of TiO_2 thin-film layers were immersed into the reactor. The process was conducted for 30 min in a dark to establish the adsorption–desorption equilibrium, which was followed by the insertion of warmed-up UV lamp in the quartz tube to initiate the photocatalytic process. The samples were taken at –30 (start of dark period), 0 (lamp turned-on), 5, 10, 15, 30, 45, 60, 75, and 90 min, filtered through Chromafil XTRA RC syringe filters (25 mm, 0.45 μm, Macherey-Nagel, Germany) and thereafter submitted to HPLC analysis. The samples for other performed analyses were taken after 90 min. All experiments were repeated at least three times and averages are reported, while the reproducibility of the experiments was >97.1%.

Table 1
Applied experimental range and the levels of independent variables applied in performed photocatalytic processes: UV-A/TiO_2(s), UV-A/TiO_2(s)/H_2O_2, and UV-A/TiO_2(i)/H_2O_2

Process parameter	Coded value	Levels		
		–1	0	1
pH	X_1	6	7	8
$\gamma(TiO_2)$ (g L^{-1})[a]	X_2	0.1	1.05	2
$[H_2O_2]$ (mM)[b]	X_3	0.1	1.05	2.0

[a]Valid for slurry processes.
[b]H_2O_2 concentration (where added).

2.4. Immobilized photocatalyst reactivation

After performed UV-A/TiO_2(i)/H_2O_2 process, glass plates with immobilized TiO_2 were air dried and subjected to thermal or chemical reactivation treatments. Thermal reactivation was performed in the laboratory furnace (LP-08 Instrumentaria, Croatia), varying the temperatures in the range T = 200°C–400°C and duration t = 120–240 min, as set by experimental plan (Table 2). UV-C/H_2O_2 process was applied for chemical reactivation of used immobilized photocatalyst. The chemical reactivation treatment was performed in the same reactor system described above, using UV-C low pressure mercury lamp, UVP-Ultra Violet Products, Cambridge, UK, instead of UV-A irradiation source. H_2O_2 concentration and treatment time were varied from 1 to 10 mM and 10 to 60 min, respectively (Table 2). Reactivated plates were used in consecutive cycle(s) of UV-A/TiO_2(i)/H_2O_2 process according to previously described procedure.

2.5. Analyses

The changes in DCF concentration were monitored by HPLC, Shimadzu, Japan, equipped with diode-array UV detector, SPD-M10AVP, Shimadzu, Japan, using EC 250/4.6 120-5 C18 column, Macherey–Nagel Nucleosil, Germany, and mobile phase CH_3OH/buffer (70:30; the buffer contained 0.15% *o*-H_3PO_4, 5% CH_3OH, and 94.85% H_2O) operating at 1.0 mL min^{-1} flow. Total organic content (TOC) of DCF aqueous solution was monitored using TOC-V_{CPN}, Shimadzu, Japan. Handylab pH/LF portable pH-meter, Schott Instruments GmbH, Mainz, Germany, was used for pH measurements. Chemical oxygen demand (COD) and biochemical oxygen demand (BOD_5) were determined by colorimetric methods using HACH DR2800 spectrophotometer, Hach Lange Co., USA. UV/VIS spectrophotometer, Lambda EZ 201, PerkinElmer, USA, was used in the determination of remained H_2O_2 concentration by modified metavanadate method [20]. In COD analysis, the results were corrected for interference by remained H_2O_2. The toxicity on *Vibrio fischeri* was examined using BioFixLumi-10 Toxicity Analyzer, Macherey-Nagel (Germany) according to ISO 11348-3. The results were expressed as effective concentration causing 50% reduction of bioluminescence (EC_{50}), and recalculated to obtain the toxicity units (TU = 100/EC_{50}%). Samples for BOD_5 and toxicity analyses containing H_2O_2 were treated prior analyses with Na_2SO_3 in excess [21]. Immobilized photocatalyst layer thickness was determined using field emission scanning electron microscope (SEM), JSM-7001F, JEOL, Japan.

Table 2
Analysis of variance (ANOVA) of the response surface model M1 predicting the DCF removal by UV-A/TiO_2(s) process

Factor (coded)	Statistical analysis				
	SS	df	MSS	F	p
Model	566.33	5	113.27	15.27	0.0241*
X_1	33.79	1	33.79	4.55	0.1225
X_1^2	0.76	1	0.76	0.10	0.7693
X_2	229.10	1	229.10	30.88	0.0115*
X_2^2	299.05	1	299.05	40.31	0.0079*
$X_1 \times X_2$	3.63	1	3.63	0.49	0.5344
Residual	22.26	3	7.42		
Total	588.58	8			

SS, sum of squares; df, degrees of dreedom; MSS, mean sum of squares.
*$p < 0.05$ are considered as significant.

2.6. Calculations

Influence of process parameters varied in photocatalytic processes (UV-A/TiO_2(s), UV-A/TiO_2(s)/H_2O_2, and UV-A/TiO_2(i)/H_2O_2) and reactivation treatments on respective yields was investigated by RSM. For that purpose, the values of studied process parameters were transferred into dimensionless coded values at three levels (–1, 0, 1; Tables 1, 5, and S1–S3), whereas DCF removal was chosen as a response. Each investigated process/treatment was described by quadratic polynomial equation representing RSM model. Models were evaluated using analysis of variance (ANOVA) and residual diagnostic tools by Design-Expert 10, StatEase Inc., USA, Statistica 12.5, Dell Inc., USA, and Mathematica 10.0 Wolfram Research, USA.

3. Results and discussion

In Fig. 1, DCF removal kinetics obtained by UV-A/TiO_2(s) and UV-A/TiO_2(s)/H_2O_2 processes, applying the conditions set by the employed full factorial design (FFD) and Box–Behnken design (BBD) of experiments (Tables S1 and S2, respectively), are presented. As can be seen, in the process conducted without oxidant (UV-A/TiO_2(s); Figs. 1(A), (C), and (E)) there are no changes in DCF concentrations observed during the initial dark period of the process. Accordingly, it can be concluded that DCF does not adsorb onto TiO_2 surface under conditions set by FFD (Tables 1 and S1). Taking into account that pH value at point of zero charge (pH_{PZC}) for AEROXIDE TiO_2 P25 lies between 5.2 and 6.7 [22–24], the results obtained by UV-A/TiO_2(s) process after initial dark period (Figs. 1(A), (C), and (E)) are not unexpected. The wide range of pH_{PZC} of TiO_2 might be explained by the method used for the preparation of TiO_2, dictating also the anatase/rutile ratio as an important factor determining pH_{PZC}, as well as the particle size [25]. Since we used AEROXIDE TiO_2 P25 with the defined anatase/rutile ratio [26], the non-adsorption effect of DCF observed in our case can be assigned to particle size. Holmberg et al. [27] stated that pH_{PZC} shifts to higher pH values as particle size decreases and vice versa. Although P25 has also defined particle size range [26], particles tend to agglomerate in slurry system, particularly in the pH range near PZC [15,25], which presumably occurred in our case. Upon illumination of TiO_2, radical species according to reactions (1)–(3) would be generated [25], and react with DCF upon diffusion in the bulk.

$$TiO_2 \xrightarrow{h\nu} h^+ + e^- \quad (1)$$

$$H_2O + h^+ \rightarrow HO\bullet + H^+ \quad (2)$$

$$O_2(aq) + e^- \rightarrow O_2\bullet^- \quad (3)$$

In such case, diffusion is a limiting factor and the overall degradation rate observed is lower than that obtained in the case when organic pollutant is adsorbed at the catalyst

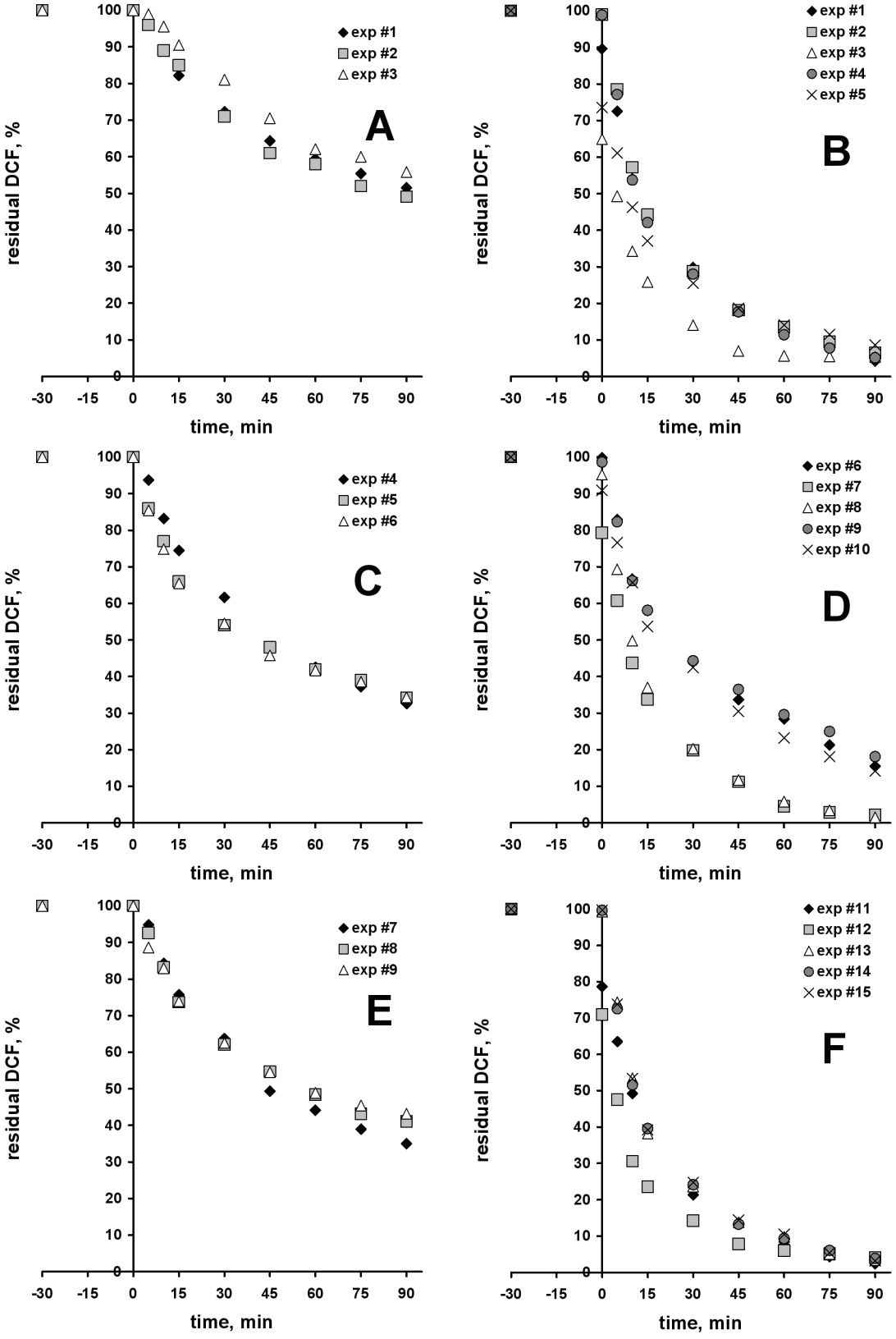

Fig. 1. DCF removal kinetics by (A), (C) and (E) UV-A/TiO_2(s) and (B), (D) and (F) UV-A/TiO_2(s)/H_2O_2 processes, obtained at experimental conditions set by FFD (for UV-A/TiO_2(s)) and BBD (UV-A/TiO_2(s)/H_2O_2) matrices (Tables S1 and S2).

surface [15,25]. As can be seen from Figs. 1(A), (C), and (E), DCF removal under UV-A irradiation obey second-order kinetics (graphical representation of calculated reaction rate constants is not presented). It can be seen that initial pH does not significantly influence the observed kinetics of DCF removal at the same TiO_2 dosages. With the lowest applied dosage (experiment no. 1–3; Table S1) DCF removal extents after 90 min ranged from 44.2% to 50.9%, while an increase in TiO_2 dosages yielded an increase in DCF removal, ranging from 59.0% to 67.4% (Figs. 1(A), (C), and (E), and Table S1). The plausible explanation can be found in the fact that with higher TiO_2 dosage more active sites for the formation of h^+/e^- pairs are available in the system. As a consequence, a higher generation of radical species in the system is expected. The addition of oxidant in the system significantly changed the process effectiveness, presumably due to two reasons. One can be easily noticed from Figs. 1(B), (D), and (F); DCF adsorption onto TiO_2 surface occurred during initial dark period of process in experiments where $pH_0 < 8$ (experimental conditions listed in Table S2). It is known from the literature that adsorption would positively influence the overall effectiveness of photocatalytic process [11,15]. This effect can be assigned to the shift of pH (after H_2O_2 addition) to slightly lower values due to the fact that H_2O_2 acts as a weak acid, which can also influence the agglomeration of TiO_2, yielding the shifting of pH_{PZC} value toward slightly higher values. Another reason for increased effectiveness of the process conducted in the presence of oxidant can be found in the process chemistry represented by reaction (4) [25,28].

$$H_2O_2 + H^+ + e^- \rightarrow HO\bullet + H_2O \quad (4)$$

In such manner, the additional source of HO• would be ensured, simultaneously decreasing the possibility for the recombination of h^+/e^-. It should be noted that the irradiation at applied wavelength (365 nm) is not effective for H_2O_2 direct photolysis yielding formation of radical species. As can be seen, DCF degradation rates in process with oxidant (Figs. 1(B), (D), and (F)) are higher than those observed in process without oxidant (Figs. 1(A), (C), and (E)). It is worth noting that kinetics altered from second order to first order. In most cases final DCF removal extents were >94%; exceptions were cases with the lowest used H_2O_2 concentrations (experiment no. 5, 6, 9, and 10; Table S2), suggesting the significance of H_2O_2 in the studied photocatalytic system.

In order to establish the significance of studied photocatalytic process parameters: pH (X_1), TiO_2 dosage (X_2), and H_2O_2 concentration (X_3) (where added) on DCF removal (Y), we applied RSM modeling approach. Hence, for each of studied processes, without (UV-A/TiO_2(s)) and with oxidant (UV-A/TiO_2(s)/H_2O_2), RSM models M1 and M2 ((5) and (6), respectively) were developed in a form of quadratic polynomials by applying multiple regression analysis (MRA) on FFD and BBD matrices and obtained values of DCF removal extents (Tables S1 and S2):

$$Y = 66.69 - 2.37 * X_1 - 0.62 * X_1^2 + 6.18 * X_2 - 12.23 * X_2^2 - 0.95 * X_1 * X_2 \quad (5)$$

$$Y = 96.49 - 1.02 * X_1 + 0.49 * X_1^2 + 0.30 * X_2 - 2.30 * X_2^2 + 5.79 * X_3 - 3.92 * X_3^2 + 0.62 * X_1 * X_2 + 1.88 * X_1 * X_3 - 1.41 * X_2 * X_3 \quad (6)$$

The significance and accuracy of M1 and M2 is evaluated using ANOVA according to standard statistical parameters (F, t, p, R^2, R_{adj}^2, and R_{pre}^2 values) and residual diagnostic tests (normal probability test, Levene's test, and constant variance test). The obtained results revealed that M1 and M2 are significant (p(M1) = 0.0241 and p(M2) = 0.0007) and accurate (R^2(M1) = 0.962 and R^2(M2) = 0.983) for studied systems (UV-A/TiO_2(s) and UV-A/TiO_2(s)/H_2O_2, respectively; Tables 2 and 3). Thus, they can be used hereinafter as a tool to enlighten the influence of studied process parameters. When comparing the RSM modeling predictions by M1 and M2 represented by 3D surface and contour plots, it can be clearly seen that significantly lower DCF removals would be obtained in the case without oxidant (Fig. 2(A)) than with oxidant (Figs. 2(B), (C), and (D)). For process without oxidant (Fig. 2(A)), TiO_2 dosage is found to be influential, which is in accordance with the previously discussed experimental results presented in Figs. 1(A), (C), and (E). This can be supported by ANOVA results provided in Table 2. As can be seen from Fig. 2(A), the model predicts that the increase in TiO_2 dosage would yield increase of DCF removal to the certain point, where further increase of TiO_2 particles in the system would result with lower process effectiveness. As described above, the positive effect of TiO_2 dosage can be contributed to the number of active sites, while negative effect can be presumably assigned to the shielding effect of TiO_2 particles present in the system [15]. 3D surface presenting combined effect of pH and TiO_2 dosage on DCF removal by UV-A/TiO_2(s)/H_2O_2 process. Fig. 2(B) indicates that changes of studied parameters within the studied range (Table 1) would not significantly influence the DCF removal. However, ANOVA results revealed that both parameters are significant (Table 3); pH contributes to the end-point through interaction effect with H_2O_2 concentration, while TiO_2 dosage contributes directly over its quadratic model term (Eq. (6)). Straightforward contribution of H_2O_2 concentration on the

Table 3
Analysis of variance (ANOVA) of the response surface model M2 predicting the DCF removal by UV-A/TiO_2(s)/H_2O_2 process

Factor	Statistical analysis				
(coded)	SS	df	MSS	F	p
Model	375.24	9	41.69	32.44	0.0007*
X_1	8.38	1	8.38	6.52	0.0510
X_1^2	0.88	1	0.88	0.69	0.4454
X_2	0.72	1	0.72	0.56	0.4885
X_2^2	19.46	1	19.46	15.14	0.0115*
X_3	267.92	1	267.92	208.43	<0.0001*
X_3^2	56.66	1	56.66	44.08	0.0012*
$X_1 \times X_2$	1.52	1	1.52	1.18	0.3261
$X_1 \times X_3$	14.09	1	14.09	10.96	0.0212*
$X_2 \times X_3$	7.91	1	7.91	6.16	0.0558
Residual	6.43	5	1.29		
Total	381.66	14			

*$p < 0.05$ are considered as significant.

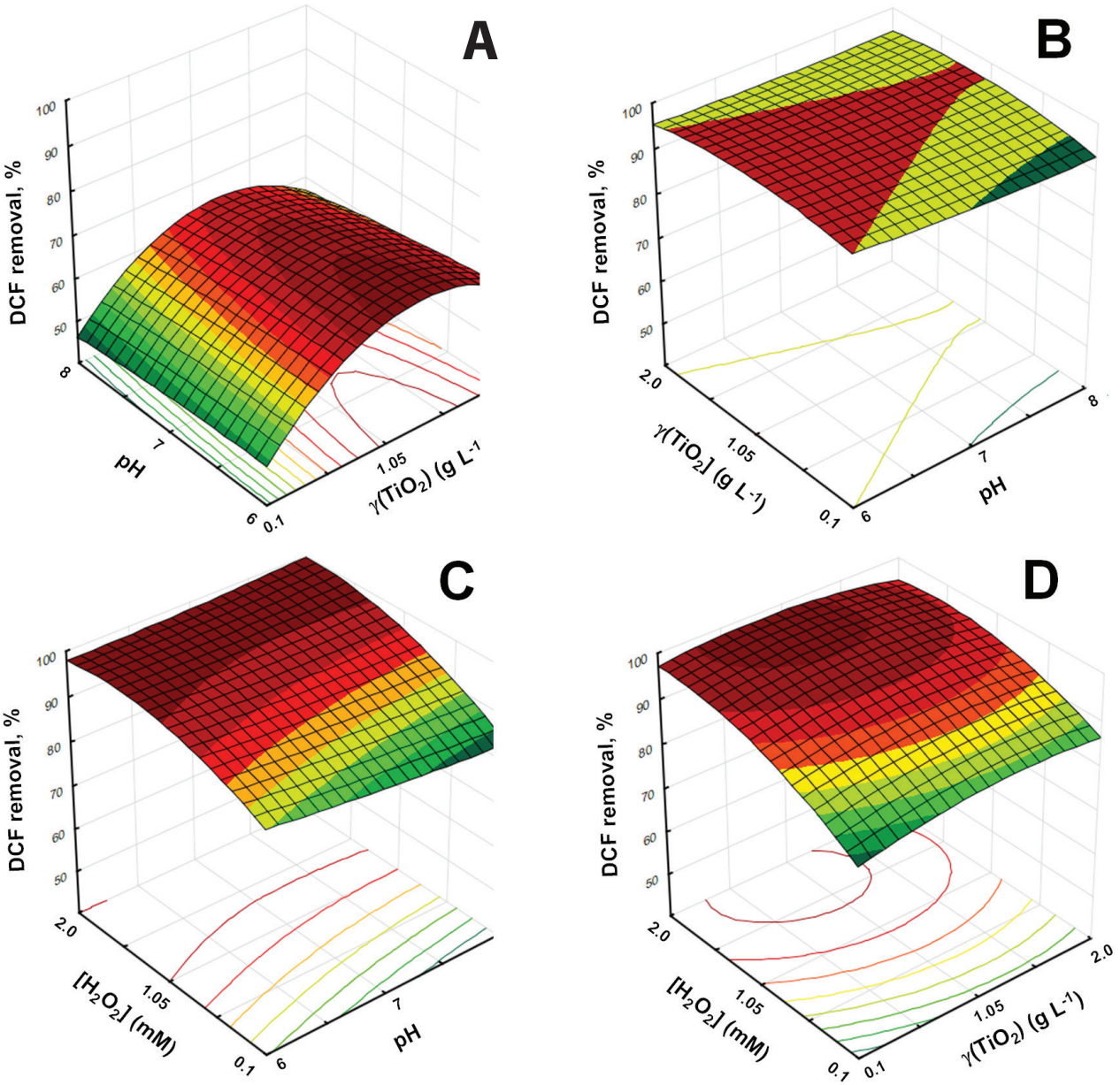

Fig. 2. 3D surface and contour plots presenting the influence of process parameters of (A) UV-A/TiO_2(s) and (B), (C) and (D) UV-A/TiO_2(s)/H_2O_2 processes through their mutual interactions on final DCF removal extents.

effectiveness of UV-A/TiO_2(s)/H_2O_2 process can be seen from 3D surfaces present in Figs. 2(C) and (D), where DCF removal rate increases with the increase of H_2O_2 concentration. This is in accordance with the previously discussed experimental results on DCF removal kinetics. Such a high influence of H_2O_2 concentration is confirmed by ANOVA results (Table 3) where three M2 model terms related to H_2O_2 possess p values <0.05 (accepted as a significance limit [29]). Developed RSM models were used to find the optimal conditions within the studied range for both processes. In that purpose, the extreme values of polynomial Eqs. (5) and (6) are found. Hence, it was determined that pH 6 is optimal for both UV-A/TiO_2(s) and UV-A/TiO_2(s)/H_2O_2 processes. However, TiO_2 dosage differs significantly; 1.33 and 0.83 g L^{-1} (along with 1.56 mM of H_2O_2) were found to optimal for maximal DCF removal of 69.5% and 99.1% by UV-A/TiO_2(s) and UV-A/TiO_2(s)/H_2O_2 processes, respectively. Such a difference can be assigned to H_2O_2 presence, contributing through reaction (4) and diminishing the recombination of h^+/e^-.

Above results showed that UV-A/TiO_2/H_2O_2 slurry process can be effectively applied for the removal of DCF from water. As proven above, the TiO_2 dosage is one of the crucial parameters in photocatalytic slurry process; it influences the reaction rate up to the achievement of the saturation level, where catalyst dosage significantly influences the light photon absorption due to increased turbidity in the system [15]. Such slurry systems usually have better mass transfer than systems operated with immobilized photocatalyst. However,

constrains of slurry systems are photocatalyst agglomeration during the treatment and the need for its post-treatment separation [15,16,28]. On the other hand, systems with immobilized catalyst may overcome above constrains and provide effective catalyst reuse (upon corresponding reactivation), but the potential limitations of such systems are related to effective mass transfer, the depth of light penetration, and the stability of immobilized catalyst toward attrition [11,15,28,30]. Accordingly, in the next step of the study UV-A/TiO_2/H_2O_2 with the immobilized photocatalyst was investigated for DCF removal. In Fig. 3, DCF removal kinetics obtained by UV-A/TiO_2(i)/H_2O_2 process at conditions set by the applied FFD of experiments (Table S3) is presented. It should be noted that in all experiments three layers of TiO_2 immobilized on glass plates were used to study the influence of pH and H_2O_2 concentration on DCF removal. According to the gravimetric measurements performed, immobilized photocatalyst amounts 1.34 g L^{-1}, while around 10 wt% pertains to used binder containing amorphous titania and silica [19]. According to the applied low-temperature method for thin-film layers fixation at glass plates, that uses heating cycles at 200°C, the crystallization of introduced amorphous titania in a form of TTIP most probably did not occur [19]. Hence, it can be considered that immobilized crystalline TiO_2 (AEROXIDE P25) amounts 1.21 g L^{-1}. As can be seen from Fig. 3, a positive influence of pH on DCF removal extent follows increasing order pH 8 < pH 7 < pH 6, regardless [H_2O_2]. It should be noted that at lower pH adsorption in the dark is favored. For instance, DCF removal by the adsorption mechanism is higher for more than 20% than in the analogues slurry process (Figs. 1 and 3, and Tables S2 and S3). This effect can be ascribed to the amorphous phase in the binder, promoting adsorptive effect, but not photocatalytic. The later is obvious from results obtained in experiment no. 1 applying UV-A/TiO_2(i)/H_2O_2 process (Fig. 3(A); conditions: pH 6 and [H_2O_2] = 0.1 mM; Tables 1 and S3) where DCF removal plateau was reached after 15 min treatment. This effect most probably occurred due to the consumption of H_2O_2 in the system during this initial period, disabling the efficient generation of HO• through reaction (4). Consequently, the recombination of h^+/e^- might be promoted, negatively contributing to the overall process effectiveness. The effect of TiO_2 surface active sites saturation by DCF adsorbed might also be taken into account. These negative effects were overcame by higher H_2O_2 concentration applied, yielding >88% DCF removal (Figs. 3(B) and (C); experiment no. 4, 7, and 8; Table S3). In the same manner as above for slurry process, RSM was applied to screen the influence of pH and H_2O_2 concentration on DCF removal, as well as to determine the optimal conditions within the studied range. Hence, the following RSM model M3 in a form of quadratic polynomial equation is generated by applying MRA on FFD matrix and obtained DCF removal extents after 90 min treatment (Table 3, Supplementary material):

$$Y = 81.48 - 9.39 * X_1 - 4.28 * X_1^2 + 11.39 * X3 - 7.19 * X_3^2 - 0.023 * X_1 * X3 \quad (7)$$

The model significance and accuracy is confirmed by ANOVA; $p = 0.0009$ and $R^2 = 0.979$, allowing its application in further study for above intended purposes (Table 4). As can

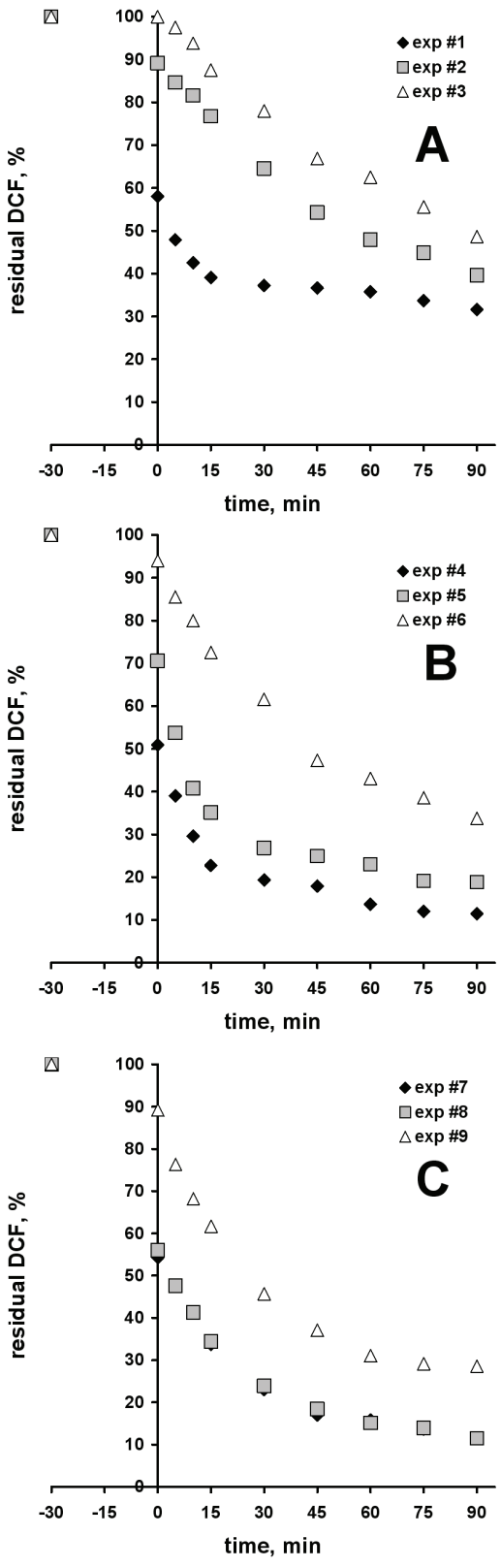

Fig. 3. DCF removal kinetics by UV-A/TiO_2(i)/H_2O_2 (A)–(C) process, obtained at experimental conditions set by FFD (Table S3), and with three layers of immobilized TiO_2 thin films.

be seen from Fig. 4, presenting mutual interactions of pH and H_2O_2 concentration on DCF removal, both studied process parameters are influential, which is additionally confirmed by ANOVA results (Table 4). However, higher influence of H_2O_2 concentration on the studied end-point (i.e., DCF removal) can be clearly seen from the curvature of 3D surface. An increase of DCF removal extent is more pronounced when increasing oxidant concentration than decreasing the pH value. It can be clearly seen that optimal conditions within the studied range are at the bottom (pH) and close to the top (H_2O_2 concentration) boundaries of the used range of parameters. Hence, M3 predicts 91.1% DCF removal at pH 6 and $[H_2O_2]$ = 1.80 mM. At these conditions the influence of catalyst dosage, varied through the number of immobilized TiO_2 thin films, was studied.

The films thickness is presented at SEM image (Fig. 5), where can be clearly seen that thickness increases linearly with the number of films, while the thickness of each layer is approximately 2.0 μm. According to Krysa et al. [31], layer thickness between 1 and 1.5 μm is enough to absorb more than 90% of UV-A radiation. Hence, it can be concluded that our thin films may be rather effective in absorbing applied irradiation.

Table 4
Analysis of variance (ANOVA) of the response surface model M3 predicting the DCF removal by UV-A/TiO_2(i)/H_2O_2 process

Factor	Statistical analysis				
(coded)	SS	df	MSS	*F*	*p*
Model	1,447.13	5	289.43	28.51	0.0099*
X_1	529.00	1	529.00	52.11	0.0055*
X_1^2	36.65	1	36.65	3.61	0.1536
X_3	778.19	1	778.19	76.65	0.0031*
X_3^2	103.29	1	103.29	10.17	0.0497*
$X_1 \times X_3$	2.16×10^{-3}	1	2.16×10^{-3}	2.13×10^{-4}	0.9893
Residual	30.46	3	10.15		
Total	1,477.59	8			

*$p < 0.05$ are considered as significant.

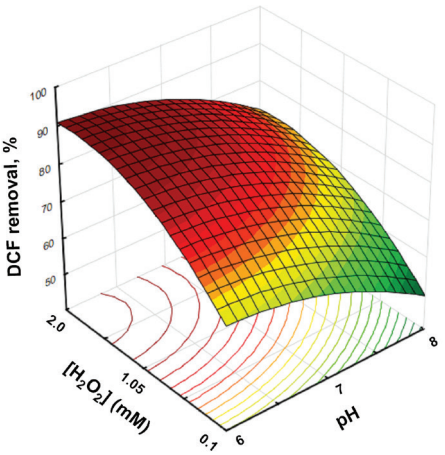

Fig. 4. 3D surface and contour plot presenting the influence of process parameters of UV-A/TiO_2(i)/H_2O_2 process through their mutual interactions on final DCF removal extents.

DCF removal kinetics obtained by UV-A/TiO_2(i)/H_2O_2 process (pH and $[H_2O_2]$ = 1.80 mM) in dependence on TiO_2 dosage represented by the number of layers of thin films is shown in Fig. 6. As can be seen, the adsorption of DCF during initial dark period increases with the number of thin-film layers. Hence, with 1 layer a negligible DCF removal can be observed, while with 4 and 5 layers 87.5 and 93.5% of initial DCF was removed (Fig. 6). Such increase in DCF removal via adsorption mechanism can be assigned to the increase of the content of amorphous phase in immobilized layer, as discussed earlier. Although very high effectiveness of UV-A/TiO_2(i)/H_2O_2 process toward DCF removal was obtained by 4 and 5 layers; after 90 min under UV-A irradiation 95.7% of DCF were removed in both cases, the immobilized films were not stable toward erosion. In those two cases a rather high attrition of immobilized TiO_2 was observed; photocatalyst mass losses of 6.5% and 7.7% were gravimetrically determined in experiments with 4 and 5 layers, respectively. Accordingly, these two cases were discarded from the further study. Considering DCF removal kinetics obtained during UV-A irradiation exposure in experiments with 1, 2, and 3 layers of TiO_2 immobilized catalyst (Fig. 6), the following can be concluded. In the cases with 1 and 2 layers, DCF removal kinetics obeyed first order yielding 47.3% and 83.2% DCF removal after 90 min treatment, respectively. On the other hand, in experiment with 3 layers, upon 45% of DCF removal obtained during initial dark period (Fig. 6), DCF removal kinetics followed the second-order kinetics. Different kinetic regimes of DCF removal regarding the number of layers can be plausibly explained by the consumption of H_2O_2 during the treatment. It was recorded that residual H_2O_2 concentration after 90 min treatment under UV-A irradiation follows decreasing order: 1 layer (0.91 mM) > 2 layers (0.42 mM) > 3 layers (0 mM). In the cases with 1 and 2 layers, ratio of TiO_2 dosage and H_2O_2 concentration ensures continuous generation of HO• under UV-A irradiation (Eq. (4)). The concentration HO•, as dominant reactive species in the system [25], is low comparing with DCF concentration, thus can be considered as constant. Hence, the rate of DCF degradation depended mainly on its concentration, yielding pseudo-first-order kinetics observed [32]. On the other hand, the complete consumption of H_2O_2 during the treatment in the case with 3 layers caused significant lowering of initial reaction rate due to decreased generation of HO• in the system through reaction (4), yielding the second-order kinetic regime. Nevertheless, the highest DCF removal (88.8%) with stable photocatalytic film is achieved in the case with 3 layers (Fig. 6), which is considered in the further study.

In Fig. 7, DCF removal kinetics, mineralization, changes in biodegradability, and toxicity toward *V. fischeri* obtained by studied photocatalytic processes conducted at conditions determined as optimal within the investigated range: UV-A/TiO_2(s) (pH 6 and $\gamma(TiO_2)$ = 1.33 g L^{-1}), UV-A/TiO_2(s)/H_2O_2 (pH 6, $\gamma(TiO_2)$ = 0.83 g L^{-1}, $[H_2O_2]$ = 1.56 mM), and UV-A/TiO_2(i)/H_2O_2 (pH 6, $[H_2O_2]$ = 1.80 mM, three layers of TiO_2 thin films) were compared. From the results presented in Fig. 7(A), it can be seen that the addition of oxidant significantly improved the effectiveness of photocatalytic process in terms of DCF removal. Decrease of parent pollutant concentration for one order of magnitude is accomplished by UV-A/TiO_2(s)/H_2O_2 in less than 45 min under UV-A irradiation, preceded with the

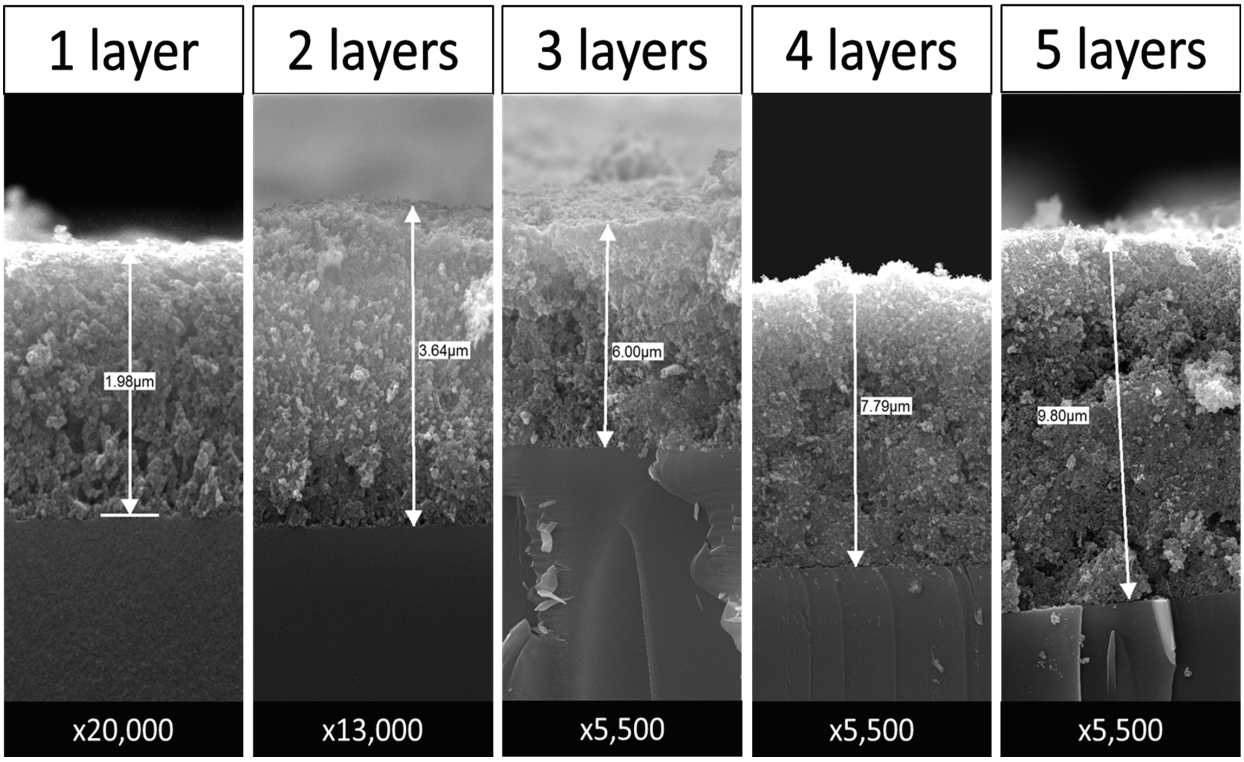

Fig. 5. SEM image of TiO_2 thin film(s) layer thickness.

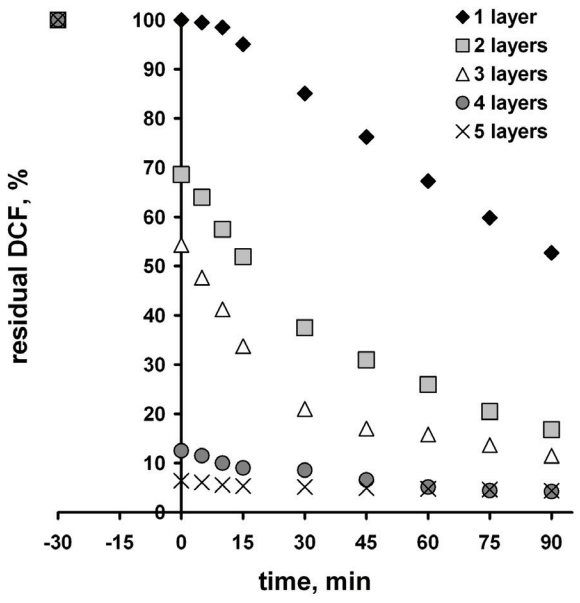

Fig. 6. DCF removal kinetics by UV-A/TiO_2(i)/H_2O_2 process in dependence on TiO_2 dosage represented through number of immobilized thin films (pH 6 and [H_2O_2] = 1.80 mM).

period of 30 min in a dark. Such effectiveness can be attributed to the combined effect of removal by adsorption and oxidative degradation in the photocatalytic system. On the other hand, process with immobilized photocatalyst yielded the same result after much longer period (i.e., 90 min), in spite of rather higher adsorption during initial dark period. In terms of TOC removal (Fig. 7(B)) UV-A/TiO_2(i)/H_2O_2 process was found to be the least effective. Such behavior can be contributed to the amorphous phase within binder used for the immobilization of TiO_2, exhibiting adsorption capacity, but without photocatalytic activity. This is reflected in biodegradability (Fig. 7(C)) whereas the lowest BOD_5/COD ratio is obtained by UV-A/TiO_2(i)/H_2O_2 process. According to the recorded toxicity toward *V. fischeri* obtained by all three studied photocatalytic processes, it can be concluded that remained organics, though non-biodegradable nature in the case of immobilized photocatalyst, are significantly less toxic than initial DCF solution. According to the above discussed results, it can be concluded that UV-A/TiO_2(s)/H_2O_2 process is the most effective for the treatment of DCF in water. However, as mentioned above, slurry systems generally suffer from limited reusability of the photocatalyst. Due to the particles size, post-treatment separation processes may significantly increase the overall treatment costs, and are characterized by significant losses of catalyst mass transferred from one cycle to another [10,15]. Therefore, the application of system with immobilized photocatalyst is generally more appropriate for practical application.

In that purpose, we investigated the possible reuse of immobilized photocatalysts. Generally, in photocatalytic water treatment, the mechanism of activity loss usually involves the adsorption of parent pollutant and/or oxidation products on the surface of the catalyst [33], while the magnitude of activity loss during consecutive usage cycles depends on the nature and concentration of the adsorbed compounds [10]. Accordingly, the loss of activity and potential reactivation methods to be applied between consecutive

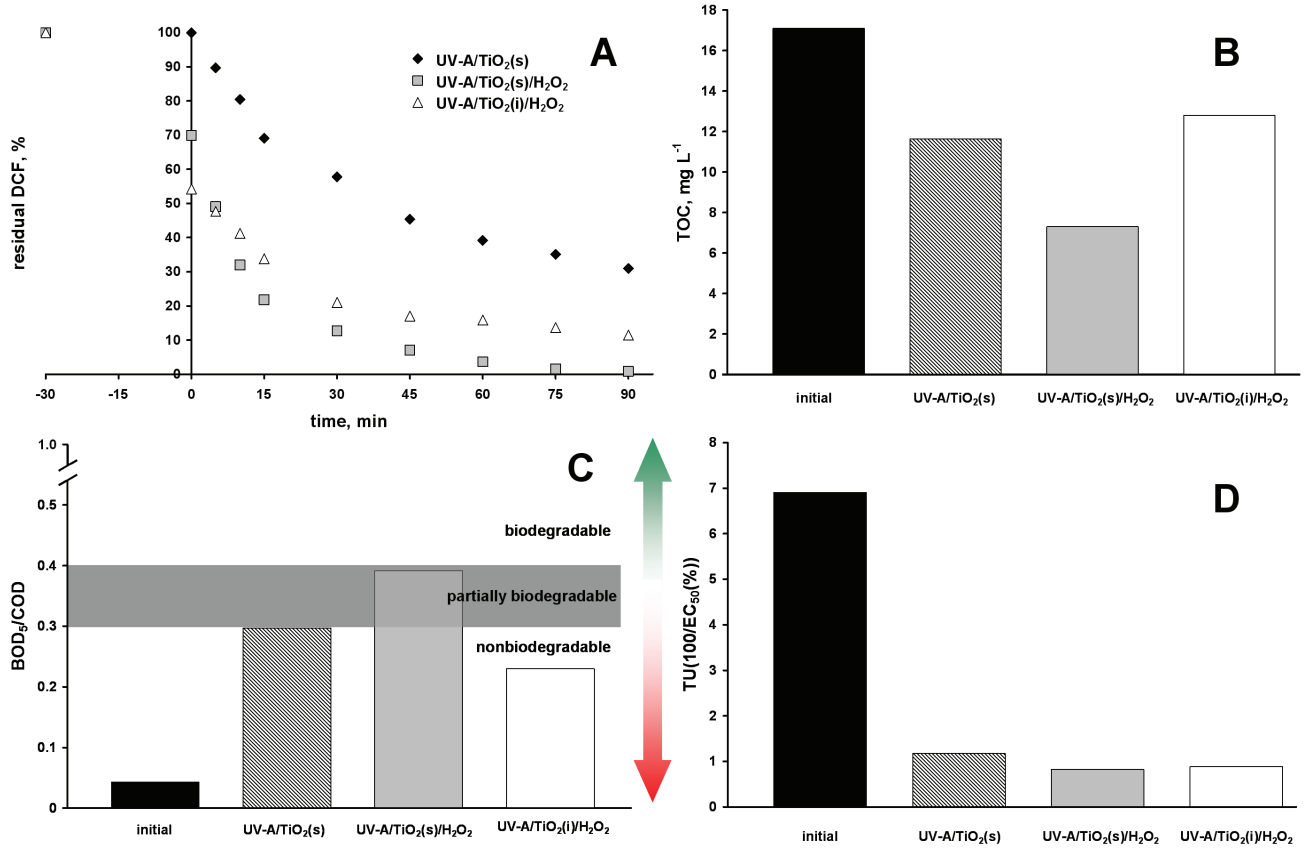

Fig. 7. Comparison of DCF removal kinetics (A), mineralization (B), changes in biodegradability (C), and toxicity toward *Vibrio fischeri* (D) obtained by UV-A/TiO_2(s) (pH 6 and $\gamma(TiO_2)$ = 1.33 g L^{-1}), UV-A/TiO_2(s)/H_2O_2 (pH 6, $\gamma(TiO_2)$ = 0.83 g L^{-1}, $[H_2O_2]$ = 1.56 mM) and UV-A/TiO_2(i)/H_2O_2 (pH 6, $[H_2O_2]$ = 1.80 mM, three layers of TiO_2 thin films).

cycles were considered for immobilized TiO_2 films in our case. Thermal and chemical treatments using UV-C/H_2O_2, were applied for photocatalyst reactivation, whereas the influence of their parameters, such as the duration of treatment and temperature or concentration of H_2O_2, is investigated on the performance of UV-A/TiO_2(i)/H_2O_2 process using such reactivated photocatalyst. In Table 5, summarized conditions applied in reactivation treatments, along with DCF removal extents obtained in reuse cycle. DCF removal kinetics obtained in reuse cycles is shown in Figs. S1 and S2. Generally, reuse cycles using thermally reactivated immobilized TiO_2 yielded significantly lower effectiveness of UV-A/TiO_2(i)/H_2O_2 process. DCF removal extents obtained after 90 min treatment ranged from 19.7% to 45.5% (Table 2) comparing with 88.8% obtained using pristine TiO_2 (Fig. 7(A)). Such results indicate that applied thermal reactivation was not efficient; activity loss was more than 50%. On the other hand, much better DCF removal was obtained using chemically reactivated TiO_2. UV-A/TiO_2(i)/H_2O_2 process effectiveness toward DCF removal in reuse cycle ranged from 59.3% to 79.0% (Table 2), that are all lower than obtained by pristine TiO_2, but also in all cases higher than obtained using thermally reactivated TiO_2.

In order to study the effects of the parameters of thermal (temperature and duration time) and chemical (H_2O_2 concentration and time of duration) reactivation on the photocatalyst activity in reuse cycle in terms of DCF removal, RSM approach was applied. By applying MRA on FFD matrices for both reactivation treatments, summarized in Table 5, and obtained system responses (i.e., DCF removal extents in reuse cycle), RSM models M4 and M5 were derived (equations are not shown). Their accuracy and significance was tested suing the using the same tools as stated above in the case of M1–M3. It was found out that both M4 and M5 possess significance for investigated thermal and chemical reactivation systems, respectively, and could accurately describe the system behavior within the investigated range of parameters (p = 0.0449 and 0.0064, R^2 = 0.942 and 0.985). 3D surface and contour plots straightforwardly demonstrating the influence of reactivation treatments parameters on the activity of TiO_2 in the reuse cycle in terms of DCF removal are presented in Fig. 8. According to the layout of 3D surface plot for thermal reactivation (Fig. 8(A)), one might conclude that both temperature and time of duration has similar influence, but that is not true. The ANOVA results revealed that only duration of treatment is contributive process parameter, whereas temperature is not. As can be seen, the lowest loss in activity, that is, highest level of photocatalyst reactivation is achieved at T = 200°C and t = 120 min. Although literature suggest that higher temperatures would lead to the effective catalyst reactivation [10] that was not occurred in our case. The plausible explanations can be found in the following

Table 5
Experimental conditions and 3^2 FFD matrices for thermal and chemical reactivation of immobilized TiO_2 photocatalyst, as well as DCF removal extents achieved in the reuse cycle

Conditions for thermal reactivation					Experimental results, ΔDCF (%)	Conditions for chemical reactivation					Experimental results, ΔDCF (%)
Experimental no.	Parameters/variables					Experimental no.	Parameters/variables				
	1		1				3		2′		
	T, °C	X_4 (coded value)	t, min	X_5 (coded value)			$[H_2O_2]$, mM	X_6 (coded value)	t, min	X_5' (coded value)	
1	200	–1	120	–1	45.47	1	1	–1	10	–1	69.30
2	200	–1	180	0	29.07	2	1	–1	35	0	66.40
3	200	–1	240	1	35.16	3	1	–1	60	1	65.66
4	300	0	120	–1	41.85	4	5.5	0	10	–1	59.25
5	300	0	180	0	25.83	5	5.5	0	35	0	62.66
6	300	0	240	1	19.37	6	5.5	0	60	1	65.20
7	400	1	120	–1	39.62	7	10	1	10	–1	63.81
8	400	1	180	0	26.47	8	10	1	35	0	68.48
9	400	1	240	1	19.71	9	10	1	60	1	79.02

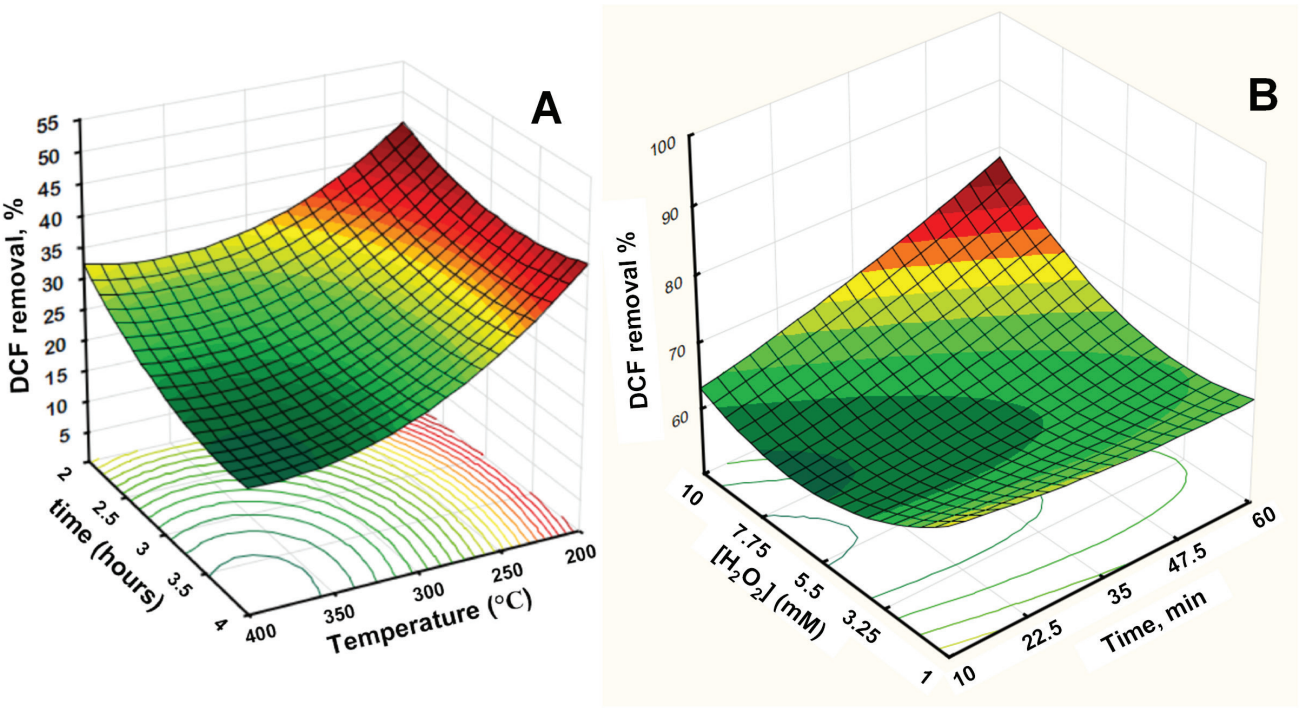

Fig. 8. 3D surface and contour plots presenting mutual interactions of parameters of thermal (A) and chemical (B) reactivation treatments on the performance of immobilized photocatalyst in the reuse cycle toward DCF removal by UV-A/TiO_2(i)/H_2O_2 (pH 6, $[H_2O_2]$ = 1.80 mM, three layers of TiO_2 thin films).

facts. A portion of our thin film was made of amorphous phase due to low-temperature method used for coating [19] and as such contributed to the adsorption of DCF removal. By thermal treatment of the immobilized films during reactivation amorphous phase was presumably converted to crystalline phase [14,16], contributing slightly to the photocatalytic activity, but that effect caused significant loss in adsorption ability of reused photocatalyst, as demonstrated in Fig. S1. Additionally, a significant loss in photocatalyst activity, observed upon reactivation at the highest temperature and duration, can be attributed to changes in photocatalyst morphology due to potential penetration of sodium from glass support, which was soda lime type. Namely, diffusion of Na^+ from soda-lime glass into TiO_2 films is dominant at T > 450°C [34], and accordingly, may occur at 400°C as well. It is proven that the presence of Na^+ would lead to the formation of Ti–O–Na bond, providing the various effects to the photocatalyst through altering its morphology [35], which

are mostly reflected as a loss in the activity of such deteriorated films [36,37]. In the case of chemical reactivation, both parameters studied were shown to be significant for predicting the end-points (i.e., DCF removal in reuse cycle). As can be clearly seen (Fig. 8(B)), the highest applied concentration of H_2O_2 and the longest period of exposure to UV-C irradiation yielded the highest DCF removal in reuse cycle. Since both TiO_2 and H_2O_2 may effectively absorb photons at applied wavelength within reactivation treatment (254 nm) [25,28], at the middle concentration of H_2O_2 a competitive absorption occurred resulting in higher activity loss than in other cases during the application of reactivated TiO_2 plates.

Upon determining the optimal conditions for both reactivation methods, the stability and activity of immobilized TiO_2 photocatalyst upon reactivation was compared through consecutive runs to pristine TiO_2 and reused (i.e., air dried) TiO_2. DCF removal kinetics through four consecutive runs was compared in Fig. 9, while UV-A/TiO_2(i)/H_2O_2 process effectiveness using reused and reactivated TiO_2 toward sum-water parameters: TOC removal, biodegradability and toxicity to *V. fischeri* is presented in Fig. 10. As can be seen, both reused and reactivated photocatalyst suffered from significant activity loss in terms of DCF removal kinetics comparing with the process using pristine TiO_2. Such effects can be assigned to the presence of remained organics, both DCF and its degradation by-products, at photocatalyst surface presumably blocking active sites. However, highest DCF removal rates were obtained after applying chemical reactivation (Fig. 9), that showed the highest efficiency in removal of adsorbed portion of

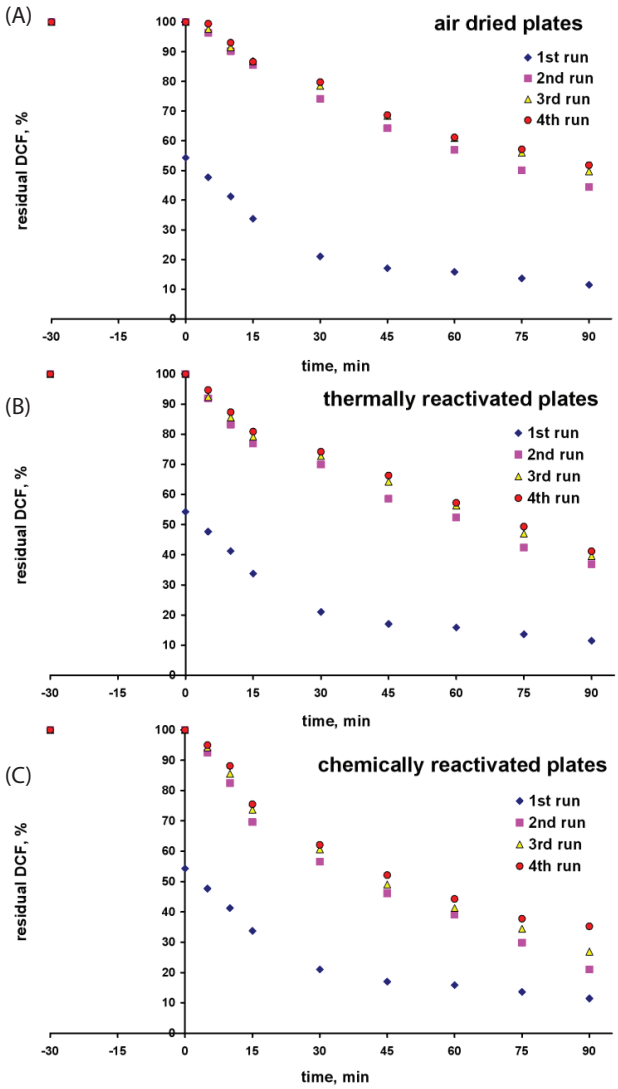

Fig. 9. Comparison of DCF removal kinetics by UV-A/TiO_2(i)/H_2O_2 (pH 6, [H_2O_2] = 1.80 mM, three layers of TiO_2 thin films) through four consecutive cycles using (A) air dried, (B) thermally reactivated (T = 200°C, t = 120 min), and (C) chemically reactivated ([H_2O_2] = 10 mM, t = 60 min) immobilized TiO_2 photocatalyst.

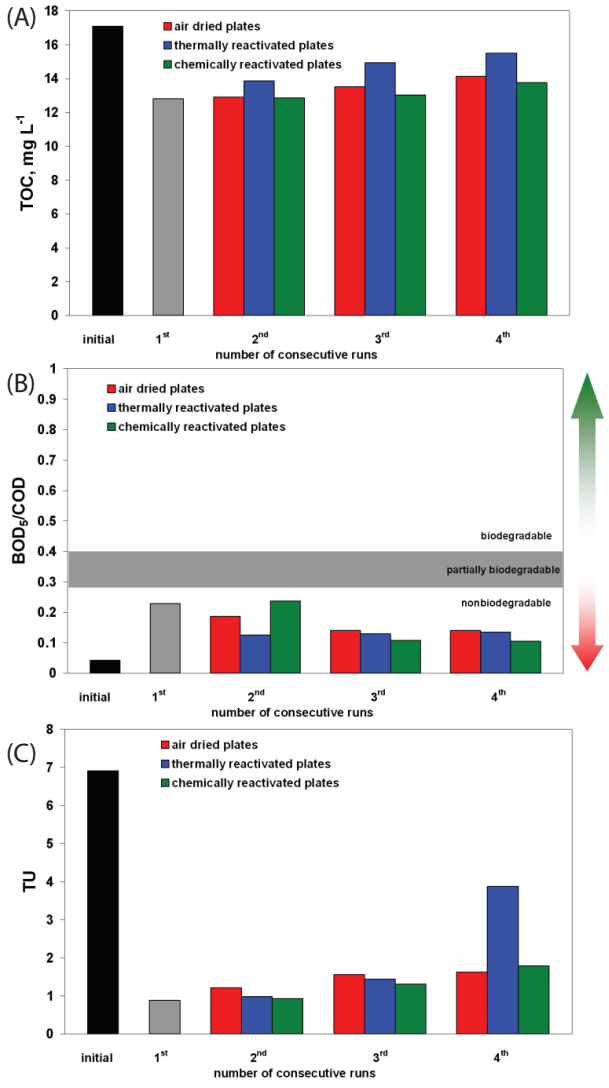

Fig. 10. (A) TOC removal, (B) biodegradability, and (C) toxicity toward *Vibrio fischeri* by UV-A/TiO_2(i)/H_2O_2 (pH 6, [H_2O_2] = 1.80 mM, three layers of TiO_2 thin films) through four consecutive cycles using air dried, thermally reactivated (T = 200°C, t = 120 min) and chemically reactivated ([H_2O_2] = 10 mM, t = 60 min) immobilized TiO_2 photocatalyst.

organics during the reactivation cycles. Considering TOC removal, efficiency decrease after each run with reused/reactivated photocatalyst can be observed (Fig. 10(A)). The highest loss of efficiency is observed after thermal reactivation, indicating that adsorbed portion of organics increases through the cycles, negatively contributing to the process effectiveness. Again, chemical treatment was shown to be the most efficient method for immobilized TiO_2 reactivation. The limitations of thermal treatment toward effective reactivation of used immobilized TiO_2 photocatalyst was reflected in biodegradability and toxicity recorded after each consecutive run (Figs. 10(B) and (C)); the obtained results are generally worse than with just reused TiO_2 plates. Most probably the thermal treatment of TiO_2 plates altered morphology of amorphous phase in photocatalyst binder, decreasing its ability to serve as adsorbent. However, this partial increase in crystallinity did not contribute to its photocatalytic activity in consecutive runs. Reused and chemically reactivated TiO_2 showed similar effectiveness regarding biodegradability and toxicity, but it should be noted that in both cases biodegradability slightly decreases, while toxicity correspondingly increases (Figs. 10(B) and (C)), indicating that photocatalysts did not retain activity through consecutive runs.

4. Conclusions

Slurry (UV-A/TiO_2(s) and UV-A/TiO_2(s)/H_2O_2) and immobilized (UV-A/TiO_2(i)/H_2O_2) photocatalytic processes were applied for the treatment of DCF and compared. The influence of operating parameters on DCF removal was investigated by applying RSM. It was found that TiO_2 dosage and H_2O_2 concentration are significant process(es) parameters, while pH was less influential within the studied range, presumably due to closeness of pH_{PZC} and corresponding rather low adsorption of DCF onto TiO_2 surface. Three applied photocatalytic processes were compared in terms of DCF removal, TOC removal, biodegradability improvement, and lowering of toxicity toward *V. fischeri*. It was found that UV-A/TiO_2(s)/H_2O_2 process provides the highest effectiveness within the investigated range of parameters: 99.1% and 57.3% of DCF and TOC removal, along with significant improvement in biodegradability in terms of BOD_5/COD (from 0.043 to 0.392) and decrease in toxicity in terms of TU (from 6.91 to 0.819). Obtained results in corresponding slurry process without H_2O_2 reflected oxidant importance on the overall process yield: 71.0% and 32.0% of DCF and TOC removals, respectively, and BOD_5/COD = 0.297 and TU = 1.176 after 90 min treatment. Although UV-A/TiO_2(i)/H_2O_2 was somewhat less effective; 88.8% and 25.2% of DCF and TOC removals, respectively, and BOD_5/COD = 0.230 and TU = 0.880, the immobilized system enabled photocatalyst reuse in consecutive treatment cycles.

Thermal and chemical treatments were applied for the reactivation of photocatalysts, while the influence of temperature, oxidant concentration, and duration of reactivation treatment on DCF removal effectiveness in reuse cycles was investigated using RSM approach. It was found that UV-A/TiO_2(i)/H_2O_2 system using chemically reactivated photocatalyst provided much better performance through four consecutive runs than systems reusing air dried or thermally reactivated photocatalysts. However, it should be noted that photocatalyst activity was lower in comparison with the case with pristine photocatalyst.

Acknowledgment

We acknowledge the financial support from Croatian Science Foundation (Project UIP-11-2013-7900; Environmental Implications of the Application of Nanomaterials in Water Purification Technologies (NanoWaP)).

References

[1] Q. Sui, X. Cao, S. Lu, W. Zhao, Z. Qiu, G. Yu, Occurrence, sources and fate of pharmaceuticals and personal care products in the groundwater: a review, Emerging Contam., 1 (2015) 14–24.
[2] T.A. Ternes, A. Joss, Human Pharmaceuticals, Hormones and Fragrances, The Challenge of Micropollutants in Urban Water Management, IWA Publishing, London, UK, 2007.
[3] EU, Directive 2013/39/EU of the European Parliament and of the Council amending Directives 2000/60/EC and 2008/105/EC as regards priority substances in the field of water policy, Off. J. Eur. Commun., 226 (2013) 1–17.
[4] Y. Zhang, S. Geißen, C. Gal, Carbamazepine and diclofenac: removal in wastewater treatment plants and occurrence in water bodies, Chemosphere, 73 (2008) 1151–1161.
[5] B. Manu, R. Mahamood, Degradation kinetics of diclofenac in water by Fenton's oxidation, J. Sustain. Energy Environ., 3 (2012) 173–176.
[6] A. Iglesias, C. Nebot, B.I. Vázquez, C. Coronel-Olivares, C.M. Franco Abuín, A. Cepeda, Monitoring the presence of 13 active compounds in surface water collected from rural areas in northwestern Spain, Int. J. Environ. Res. Public Health, 11 (2014) 5251–5272.
[7] N. Vieno, M. Sillanpää, Fate of diclofenac in municipal wastewater treatment plant – a review, Environ. Int., 69 (2014) 28–39.
[8] H. Yu, E. Nie, J. Xu, S. Yan, W.J. Cooper, W. Song, Degradation of diclofenac by advanced oxidation and reduction processes: kinetic studies, degradation pathways and toxicity assessments, Water Res., 47 (2013) 1909–1918.
[9] M.I. Litter, R.J. Candal, J.M. Meichtry, Advanced Oxidation Technologies: Sustainable Solutions for Environmental Treatments, CRC Press, Taylor and Francis, London, UK, 2014.
[10] N. Miranda-García, S. Suárez, M.I. Maldonado, S. Malato, B. Sánchez, Regeneration approaches for TiO_2 immobilized photocatalyst used in the elimination of emerging contaminants in water, Catal. Today, 230 (2014) 27–34.
[11] S. Salaeh, D. Juretic Perisic, M. Biosic, H. Kusic, S. Babic, U. Lavrencic Stangar, D.D. Dionysiou, A. Loncaric Bozic, Diclofenac removal by simulated solar assisted photocatalysis using TiO_2-based zeolite catalyst; mechanisms, pathways and environmental aspects, Chem. Eng. J., 304 (2016) 289–302.
[12] Y. He, N.B. Sutton, H.H.H. Rijnaarts, A.A.M. Langenhoff, Degradation of pharmaceuticals in wastewater using immobilized TiO_2 photocatalysis under simulated solar irradiation, Appl. Catal., B, 182 (2016) 132–141.
[13] D. Kanakaraju, B.D. Glass, M. Oelgemöller, Titanium dioxide photocatalysis for pharmaceutical wastewater treatment, Environ. Chem. Lett., 12 (2014) 27–47.
[14] M. Pelaez, N.T. Nolan, S.C. Pillai, M.K. Seery, P. Falaras, A.G. Kontos, P.S.M. Dunlop, J.W.J. Hamilton, J.A. Byrne, K. O'Shea, M.H. Entezari, D.D. Dionysiou, A review on the visible light active titanium dioxide photocatalysts for environmental applications, Appl. Catal., B, 125 (2012) 331–349.
[15] M.N. Chong, B. Jin, C.W.K. Chow, C. Saint, Recent developments in photocatalytic water treatment technology: a review, Water Res., 44 (2010) 2997–3027.
[16] A.O. Ibhadon, P. Fitzpatrick, Heterogeneous photocatalysis: recent advances and applications, Catalysts, 3 (2013) 189–218.

[17] M.A. Lazar, S. Varghese, S.S. Nair, Photocatalytic water treatment by titanium dioxide: recent updates, Catalysts, 2 (2012) 572–601.
[18] A.Y. Shan, T.I. Mohd Ghazi, S.A. Rashid, Immobilisation of titanium dioxide onto supporting materials in heterogeneous photocatalysis: a review, Appl. Catal., A, 389 (2010) 1–8.
[19] M. Kete, E. Pavlica, F. Fresno, G. Bratina, U. Lavrencic Stangar, Highly active photocatalytic coatings prepared by a low-temperature method, Environ. Sci. Pollut. Res., 21 (2014) 11238–11249.
[20] R. Nogueira, M.C. Oliveira, W.C. Paterlini, Simple and fast spectrophotometric determination of H_2O_2 in photo-Fenton reactions using metavanadate, Talanta, 66 (2005) 86–91.
[21] M.J. Farre, M.I. Franch, J.A. Ayllon, J. Peral, X. Domenech, Biodegradability of treated aqueous solutions of biorecalcitrant pesticides by means of photocatalytic ozonation, Desalination, 211 (2007) 22–33.
[22] N.T. Boncagni, J.M. Otaegui, E. Warner, T. Curran, J. Ren, M.M. Fidalgo de Cortalezzi, Exchange of TiO_2 nanoparticles between streams and streambeds, Environ. Sci. Technol., 43 (2009) 7699–7705.
[23] V. Buscio, S. Brosillon, J. Mendret, M. Crespi, C. Gutiérrez-Bouzán, Photocatalytic membrane reactor for the removal of C.I. disperse Red 73, Materials, 8 (2015) 3633–3647.
[24] M. Zeng, Influence of TiO_2 surface properties on water pollution treatment and photocatalytic activity, Bull. Korean Chem. Soc., 34 (2013) 953–956.
[25] P. Pichat, Photocatalysis and Water Purification: From Fundamentals to Recent Applications, Wiley, Weinheim, Germany, 2013.
[26] Evonik Industries, AEROXIDE®, AERODISP® and AEROPERL® Titanium Dioxide as Photocatalyst, Technical Information 1243, Available at: https://www.aerosil.com/sites/lists/IM/Documents/TI-1243-Titanium-Dioxide-as-Photocatalyst-EN.pdf (Accessed December 18, 2016).
[27] J.P. Holmberg, E. Ahlberg, J. Bergenholtz, M. Hassellöv, Z. Abbas, Surface charge and interfacial potential of titanium dioxide nanoparticles: experimental and theoretical investigations, J. Colloid Interface Sci., 407 (2013) 168–176.
[28] S. Malato, P. Fernandez-Ibanez, M.I. Maldonado, J. Blanco, W. Gernjak, Decontamination and disinfection of water by solar photocatalysis: recent overview and trends, Catal. Today, 147 (2009) 1–59.
[29] M. Dopar, H. Kusic, N. Koprivanac, Treatment of simulated industrial wastewater by photo-Fenton process: part I. The optimization of process parameters using design of experiments (DOE), Chem. Eng. J., 173 (2011) 267–279.
[30] M. Kovacic, S. Salaeh, H. Kusic, A. Suligoj, M. Kete, M. Fanetti, U. Lavrencic Stangar, D.D. Dionysiou, A. Loncaric Bozic, Solar-driven photocatalytic treatment of diclofenac using immobilized TiO_2-based zeolite composites, Environ. Sci. Pollut. Res., 23 (2016) 17982–17994.
[31] J. Krysa, M. Keppert, G. Waldner, J. Jirkovsky, Immobilized particulate TiO_2 photocatalysts for degradation of organic pollutants: effect of layer thickness, Electrochim. Acta, 50 (2005) 5255–5260.
[32] K.A. Connors, Chemical Kinetics: The Study of Reaction Rates in Solution, Wiley, New York, USA, 1990.
[33] D. Panayotov, P. Kondratyuk, J.T. Yates Jr., Photooxidation of a mustard gas simulant over TiO_2–SiO_2 mixed-oxide photocatalyst: site poisoning by oxidation products and reactivation, Langmuir, 20 (2004) 3674–3678.
[34] K. Surekha, S. Sundararajan, Self-cleaning Glass, M. Aliofkhazraei, Ed. Anti-abrasive Nanocoatings: Current and Future Applications, Elsevier, Amsterdam, Netherlands, 2015, pp. 81–104.
[35] H. Xie, N. Li, B. Liu, J. Yang, X. Zhao, Role of sodium ion on TiO_2 photocatalyst: influencing crystallographic properties or serving as the recombination center of charge carriers? J. Phys. Chem. C, 120 (2016) 10390–10399.
[36] U. Lavrenčič Štangar, U. Černigoj, P. Trebše, K. Maver, S. Gross, Photocatalytic TiO_2 coatings: effect of substrate and template, Monatsh. Chem., 137 (2006) 647–655.
[37] C. Guillard, B. Beaugiraud, C. Dutriez, J.M. Herrmann, H. Jaffrezic, N. Jaffrezic-Renault, M. Lacroix, Physicochemical properties and photocatalytic activities of TiO_2-films prepared by sol–gel methods, Appl. Catal., B, 39 (2002) 331–342.

Supplementary material

Table S1
Full factorial design matrix for UV-A/TiO_2(s) process with two independent variables expressed in coded units and experimentally obtained and RSM modeled DCF removal

Experimental no.	X_1	X_2	DCF removal, %	
			Experiment	Predicted by model
1	–1	–1	48.51	49.09
2	0	–1	50.9	48.29
3	1	–1	44.21	46.25
4	–1	0	67.44	68.45
5	0	0	65.78	66.69
6	1	0	65.63	63.7
7	–1	1	64.94	63.35
8	0	1	58.95	60.65
9	1	1	56.82	56.7

Table S2
Box–Behnken design matrix for UV-A/TiO_2(s)/H_2O_2 process with three independent variables expressed in coded units and experimentally obtained and RSM modeled DCF removal

Experimental no.	X_1	X_2	X_3	DCF removal, %	
				Experiment	Predicted by model
1	–1	–1	0	95.77	96.03
2	1	–1	0	93.52	92.75
3	–1	1	0	94.61	95.39
4	1	1	0	94.84	94.58
5	–1	0	–1	91.36	90.18
6	1	0	–1	84.52	84.38
7	–1	0	1	97.86	98.00
8	1	0	1	98.52	99.71
9	0	–1	–1	81.87	82.79
10	0	1	–1	85.80	86.20
11	0	–1	1	97.58	97.17
12	0	1	1	95.88	94.96
13	0	0	0	96.55	96.49
14	0	0	0	96.14	96.49
15	0	0	0	96.80	96.49

Table S3
Full factorial design matrix for UV-A/TiO_2(i)/H_2O_2 process with two independent variables expressed in coded units and experimentally obtained and RSM modeled DCF removal

Experimental no.	X_1	X_3	DCF removal, %	
			Experiment	Predicted by model
1	–1	–1	68.35	67.99
2	0	–1	60.42	62.90
3	1	–1	51.37	49.25
4	–1	0	88.50	86.59
5	0	0	81.16	81.48
6	1	0	66.21	67.81
7	–1	1	88.53	90.81
8	0	1	88.49	85.68
9	1	1	71.46	71.99

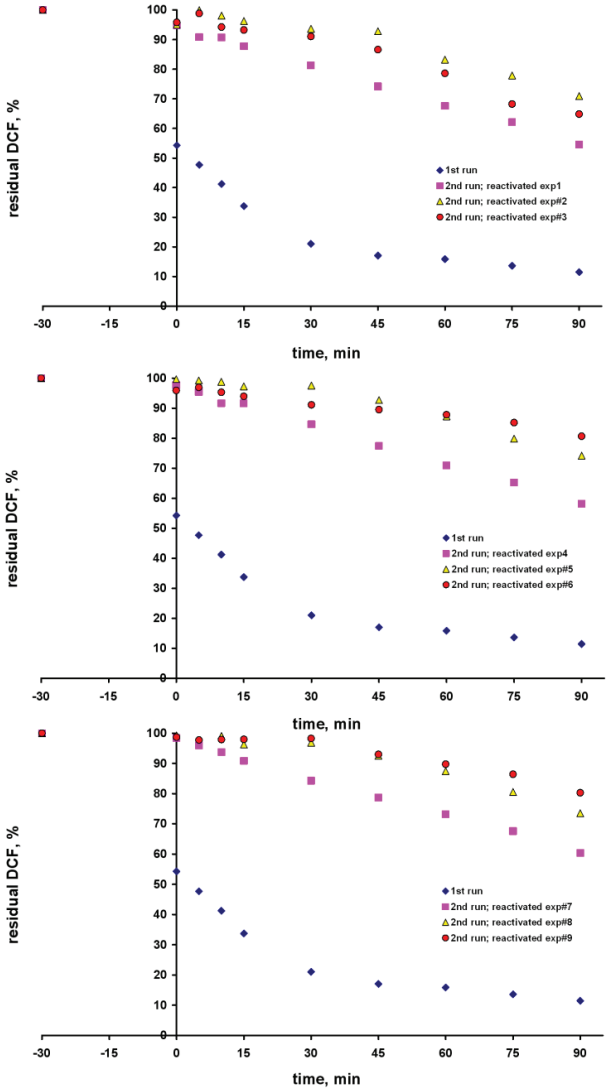

Fig. S1. DCF removal kinetics by UV-A/TiO_2(i)/H_2O_2 (pH 6, [H_2O_2] = 1.80 mM, three layers of TiO_2 thin films) using thermally reactivated photocatalyst at conditions set in Table 2.

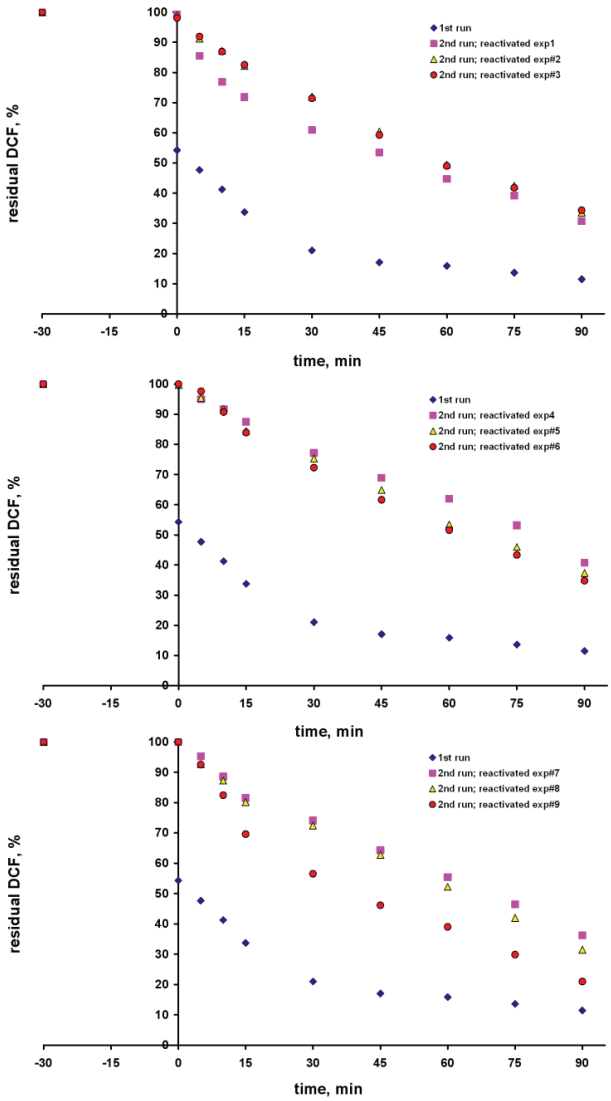

Fig. S2. DCF removal kinetics by UV-A/TiO_2(i)/H_2O_2 (pH 6, [H_2O_2] = 1.80 mM, three layers of TiO_2 thin films) using chemically reactivated photocatalyst at conditions set in Table 2.